Optimal LQG controller design for self-balancing two-wheeled vehicle stabilization

Gonzalo Gabriel Fernandez
Facultad de Ingeniería, Universidad Nacional de Cuyo

***Abstract*—Formulation of a mathematical model of a self-balancing two-wheeled vehicle. Implementation of mechanical model in Simscape Multibody with 3D visualization. Design of linear quadratic Gaussian LQG controller, combination of linear quadratic regulator LQR and linear quadratic observer (Kalman filter), for stabilization and tracking of translation setpoints. Controller performance analysis for initial angles different from 0 and thrust forces on the vehicle.**

I. Introduction

In the last decades there have been great advances in mobile robotics, leading to competent robots that are used in different industries. Land mobile robots are widely used, for example, for cargo transportation, and in their development two goals are pursued: the ability to move quickly and efficiently, and the ability to circumvent obstacles present in their environment.

In general, terrestrial robots can be classified according to their form of locomotion in two main groups: those based on legs and those based on some type of rotating element such as wheels or caterpillars. Leg-based robots are characterized by their great maneuverability to avoid obstacles, but they move relatively slowly due to the complexity involved in each of their movements. In contrast, wheel-based robots can move quickly but can only overcome obstacles if they are small and the wheel does not lose contact with the ground.

In the search for a terrestrial robot that stands out for its agility and versatility, projects such as the Ascento robot, whose configuration combines two articulated legs with wheels at both ends, have emerged. In this way, the wheels allow it to move at high speed while the legs give it the freedom to negotiate irregularities in the terrain or even jump off the ground.

One of the main characteristics of this configuration is the fact that it has only two wheels and the center of mass of the robot above its axis of rotation, which makes it an inherently unstable structure. A controller is proposed to solve the stabilization problem of a simplified version of such a robot where leg motion is not considered, Figure 1.

The vehicle's actuators are two DC motors, each with a gearbox coupled to the corresponding wheel. The sensors available to the system are incremental encoders that measure the angular position of the shaft of each motor, and an IMU (inertial measurement unit) consisting of an accelerometer and a gyroscope mounted on the vehicle chassis in such a way as to estimate its orientation.

For the aforementioned task, the design of an optimal controller is proposed. Optimal control is a particular branch of modern control, which allows to obtain systems that are not only stable and meet the requirements of classical control (transient response with certain characteristics, disturbance rejection, no steady state error, robustness of the controller to model uncertainty, etc.), but are also the best possible solution of a particular type. Linear optimal control is a special type of optimal control where the plant to be controlled is assumed to be linear. Such linear controllers are obtained by working with quadratic performance indices and are called linear quadratic (LQ)[1].

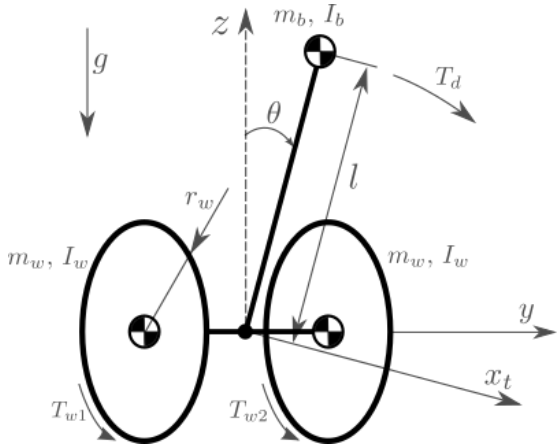

Fig. 1. Simplified schematic of the physical system

Given the mechanical power of the actuators and the characteristics of the sensors that were selected as reference, it is desired to know what performance can be obtained by implementing an LQG controller for vehicle stabilization, in an initial design stage with a *model-in-the-loop* strategy.

II. Design process and requirements to be met by the vehicle controller

Figure 20 shows a diagram summarizing the design process of a controller. In light blue the stages discussed in the work are highlighted:

1) The definition of the requirements to be met by the controller,
2) the formulation of the mathematical model of the plant,
3) the approach of a control by complete feedback of state,
4) the design of a complete state observer.

It is necessary then, to define the requirements that the controller must fulfill to discern if its operation is correct or not. For this purpose, the objective of the work is to obtain a controller that allows the vehicle, at least, to follow a sinusoidal

position setpoint with an amplitude of half a meter and a period of 15 seconds, remaining stable along the entire path. The tolerance admitted in time is 1 second, and in translation an error of $\pm 10cm$ is admitted.

At the end of the work, a systematic analysis of the design process is obtained, and the necessary software is available so that, once the mechanical requirements of the vehicle for a specific application have been defined, the parameters of the initial stages (including the requirements) can be changed and the corresponding controller can be quickly obtained.

III. Formulation of the Mathematical Model of the Vehicle

A. Description of the simplified physical model

It is desired to obtain the mathematical model of the system from physical relations, for which a series of considerations are made. The first one is the assumption that the wheels of the vehicle do not slide with the ground, therefore:

$$x_t = r_w \phi \qquad \dot{x}_t = r_w \dot{\phi} \tag{1}$$

Where x_t is the translation coordinate of the system with respect to a fixed frame of reference in the environment, phi is the angle of rotation of the wheels and r_w is the radius of the wheels. Since the present work seeks to solve the vehicle stabilization problem and does not analyze the navigation problem in the environment, where it would be necessary to characterize the position and orientation in the xy plane, both wheels are considered to be driven in the same way and synchronously rotate the same angle at the same angular velocity. The wheels have a given mass m_w and moment of inertia I_w with respect to their axis of rotation, and the output of the gearbox of the motors applies a total torque T_w equal to the sum of the torque of each motor on its corresponding coupled wheel.

The vehicle body is physically modeled as an inverted pendulum with point mass m_b located at the center of mass of the chassis, and moment of inertia I_b with respect to the wheel axis (figure 1). The coordinates of this point are described by the following equations:

$$\begin{cases} x_{cm} = l \sin\theta + r_w \phi \\ z_{cm} = l \cos\theta \end{cases} \tag{2}$$

Where l is the length of the segment joining the axis of the wheels and the center of mass, and $theta$ is the angle formed by this segment with a vertical plane, perpendicular to the ground, which crosses the axis of the wheels.

Any perturbation on the vehicle chassis is modeled as a torque T_d applied on the pivot point of the pendulum, i.e., the axis of the wheels.

Table I summarizes the parameters along with the corresponding values used in the vehicle model.

Parameter	Value	Description
r_w	32mm	Wheel radius
m_w	0.064Kg	Wheel mass
I_w	2.787×10^{-5}Kgm^2	Wheel moment of inertia with respect to its axis of rotation
b_w	$0.01 Nm^s/_{rad}$	Contact damping wheel-ground
m_b	0.5Kg	Chassis mass
I_b	0.0029Kgm^2	Moment of inertia of chassis relative to wheel axis
l	$0.06m$	Length of the segment joining the axis of the wheels and the center of mass of the chassis

TABLE I
PARAMETERS OF THE MODELED VEHICLE

B. Dynamic model, equations of motion

The equations of motion are obtained from an energetic approach following the Lagrangian formulation. For this it is necessary to obtain the kinetic and potential energy expressions of the system under study.

The kinetic energy of the wheel, 1 or 2 since they are considered identical, is:

$$E_{w(1,2)} = \frac{1}{2} m_w \dot{x}_t^2 + \frac{1}{2} I_w \dot{\phi}^2 \tag{3}$$

Being two wheels, and applying the relation of the equation 1, the following kinetic energy expression is obtained:

$$E_w = E_{w1} + E_{w2} = \left(m_w + \frac{I_w}{r_w^2} \right) \dot{x}_t^2 \tag{4}$$

The kinetic energy of the pendulum is given by:

$$E_b = \frac{1}{2} m_b v_b^2 + \frac{1}{2} I_b \dot{\theta}^2 \tag{5}$$

Deriving the equation 2, we obtain the velocity of the center of mass in its respective components x and z:

$$\begin{cases} \dot{x}_{cm} = l\dot{\theta}\cos\theta + r_w\dot{\phi} = l\dot{\theta}\cos\theta + \dot{x}_t \\ \dot{z}_{cm} = -l\dot{\theta}\sin\theta \end{cases} \tag{6}$$

The linear velocity of the center of mass of the pendulum v_b is given by:

$$v_b = \sqrt{\dot{x_{CM}}^2 + \dot{z_{CM}}^2} \tag{7}$$

The potential energy of the wheels is zero, since their center is considered to remain at a constant height z equal to their radius, so:

$$V_w = 0 \tag{8}$$

The potential energy of the pendulum is of the following form:

$$V_b = m_b g l \cos\theta \tag{9}$$

Where g is the acceleration in z due to gravity.

In the simplified model of the trolley-pendulum system only that produced by the friction b_w between the wheels and the floor is considered as dissipated energy:

$$D = \frac{1}{2} b_w \dot{\phi}^2 \times 2 = \frac{b_w}{r_w^2} \dot{x}_t^2 \tag{10}$$

Multiplied by two to be equal for both wheels.

The total kinetic energy being the sum of the kinetic energy of the wheels and that of the pendulum $E = E_w + E_b$, and the total potential energy the potential energy of the wheels and the pendulum $V = V_w + V_b$, the Lagrangian is defined as the difference between the kinetic and potential energy $L = E - V$.

Then, the dynamic equations describing the motion of the system are obtained through the Euler-Lagrange equations, of the form:

$$\frac{d}{dt}\left(\frac{\partial L}{\partial \dot{q}_i}\right) - \frac{\partial L}{\partial q_i} = Q_i - \frac{\partial D}{\partial \dot{q}_i} \tag{11}$$

Where q_i are the generalized coordinates of the system (equation 12), which fully describe the position and orientation of the vehicle: x_t the translation coordinate and θ its angle of inclination with respect to the vertical.

$$\underline{q} = \begin{bmatrix} q_1 \\ q_2 \end{bmatrix} = \begin{bmatrix} x_t \\ \theta \end{bmatrix} \tag{12}$$

And where Q_i are the generalized forces (equation 13), in this case the torques applied to each wheel T_{w1} and T_{w2} and the perturbations on the vehicle chassis T_d.

$$\bar{Q} = \begin{bmatrix} Q_1 \\ Q_2 \end{bmatrix} = \begin{bmatrix} F_x \\ M_0 \end{bmatrix} = \begin{bmatrix} T_w/r_w \\ -T_w + T_d \end{bmatrix} \tag{13}$$

The dynamic equations of motion obtained for the trolley-pendulum system are as follows:

$$\begin{aligned} m_{eq}\ddot{x}_t + m_b l\cos\theta\ddot{\theta} - m_b l\dot{\theta}^2\sin\theta + \tfrac{2b_w}{r_w^2}\dot{x}_t = \tfrac{1}{r_w}T_w \\ m_b l\cos\theta\ddot{x}_t + I_{eq}\ddot{\theta} - m_b g l\sin\theta = -T_w + T_d \end{aligned} \tag{14}$$

Where,

$$\begin{aligned} m_{eq} &= m_b + 2m_w + \frac{2I_w}{r_w^2} \\ I_{eq} &= I_b + m_b l^2 \end{aligned}$$

It can be identified that both equations are nonlinear, and can be expressed in matrix form of the form:

$${}^{NL}\mathbb{E}(\underline{q})\cdot\ddot{\underline{q}} + \overline{h(\underline{q},\dot{\underline{q}})} = \mathbb{H}_T\cdot\overline{u} \tag{15}$$

Where,

$${}^{NL}\mathbb{E}(\underline{q}) = \begin{bmatrix} m_b + 2m_w + \frac{2I_w}{r_w^2} & m_b l\cos\theta \\ m_b l\cos\theta & I_b + m_b l^2 \end{bmatrix} \tag{16}$$

$$\overline{h(\underline{q},\dot{\underline{q}})} = \begin{bmatrix} -m_b l\dot{\theta}^2\sin\theta + \frac{2b_w}{r_w^2}\dot{x} \\ -m_b g l\sin\theta \end{bmatrix} \tag{17}$$

$$\mathbb{H}_T = \begin{bmatrix} \frac{1}{r_w} & 0 \\ -1 & 1 \end{bmatrix} \qquad \overline{u} = \begin{bmatrix} T_w \\ T_d \end{bmatrix} \tag{18}$$

C. Nonlinear state-space model

We arrive at a state-space representation of the model, defining the state vector as:

$$\underline{x} = \begin{bmatrix} \underline{q} \\ \dot{\underline{q}} \end{bmatrix} = \begin{bmatrix} x_t & \theta & \dot{x}_t & \dot{\theta} \end{bmatrix}^T \tag{19}$$

It can be seen that the dimension of the state vector, and hence the order of the model, is $n = 4$.

The state-space representation of the nonlinear model will be of the form:

$$\dot{\underline{x}} = \overline{f(\underline{x},\underline{u},t)} \tag{20}$$

From the equation 14, the following matrix equation can be obtained:

$$\begin{aligned} \dot{\underline{x}} &= \begin{bmatrix} \dot{\underline{q}} = \begin{bmatrix} \dot{q}_1 \\ \dot{q}_2 \end{bmatrix} \\ -{}^{NL}\mathbb{E}(\underline{q})^{-1}\cdot\overline{h(\underline{q},\dot{\underline{q}})} \end{bmatrix} + \begin{bmatrix} 0 \\ 0 \\ {}^{NL}\mathbb{E}(\underline{q})^{-1}\cdot\mathbb{H}_T \end{bmatrix}\cdot\underline{u} \\ \underline{x}_0 &= \begin{bmatrix} x_{t0} & \theta_0 & \dot{x}_{t0} & \dot{\theta}_0 \end{bmatrix}^T \end{aligned} \tag{21}$$

Where $\underline{x}_0$ are the initial conditions of the system.

The design of the nonlinear model in MATLAB Simulink can be seen in figure 21. In order to verify the mathematical model obtained, the response of the nonlinear model to a null input and an initial tilt angle θ_0 assigned a value close to zero ($\theta_0 = 0.1rad$) was analyzed. In figure 2 is such response, where in blue can be observed the variable x_t, which has a small oscillation and remains at 0, and in red the variable θ which when given an initial value, however small, is taken out of its unstable equilibrium condition at $\theta = 0$ and oscillates by damping and settling in its stable equilibrium condition at $\theta = \pi$. Physically the robot cannot reach the $\theta = \pi$ condition as it would first impact the ground, however, it is useful to illustrate that the mathematical model is correct.

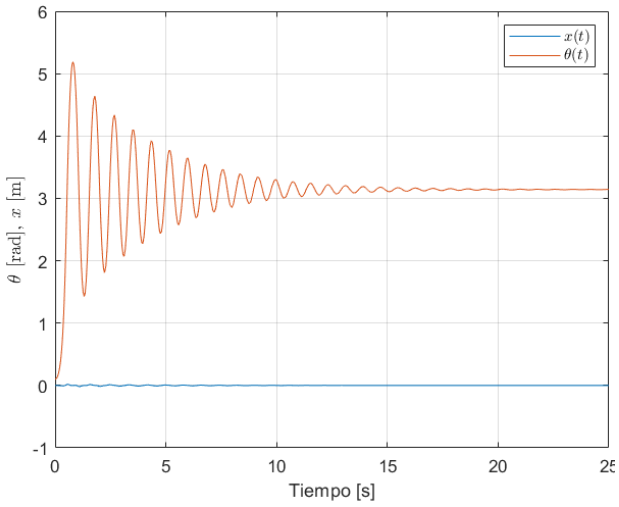

Fig. 2. Open-loop nonlinear model response to zero input and initial angle $\theta_0 = 0.1rad$

D. Simplified linear time invariant model LTI

The linearization of the system is performed around an operating point that is chosen in an equilibrium configuration. Mathematically the system has two equilibrium points at $theta$, one stable for $theta = 0$ and one unstable for $theta = 0$, both with $theta = 0$. Physically, and the one of interest in the application, is the unstable equilibrium point where $\theta = 0$, i.e., where the pendulum swings inverted. The translation coordinate x_t is free since it does not contribute nonlinearities to the model (the system can stabilize at any coordinate x_t).

The Jacobian of the nonlinear model must be obtained in order to proceed to linearize at the operating point $x_t = 0$. However, since the procedure is very extensive, for practical

purposes the following approximations are made for small angles leading to the same result:

$$\cos\Theta_0 \approx 1 \qquad \sin\Theta_0 \approx \Theta_0 \qquad \dot{\Theta}_0 \approx 0 \tag{22}$$

And linearizing the equations **??**, we obtain the following linear equations:

$$\begin{aligned} m_{eq}\ddot{x}_t + m_b l\ddot{\theta} + \tfrac{2b_w}{r_w^2}\dot{x}_t &= \tfrac{1}{r_w}T_w \\ m_b l\ddot{x}_t + I_{eq}\ddot{\theta} - m_b g l\theta &= -T_w + T_d \end{aligned} \tag{23}$$

The equation 23 can be expressed in matrix form as:

$$\mathbb{E}\cdot\ddot{\underline{q}} + \mathbb{F}\cdot\dot{\underline{q}} + \mathbb{G}\cdot\underline{q} = \mathbb{H}_T\cdot\overline{u} \tag{24}$$

Where,

$$\mathbb{E} = \begin{bmatrix} m_{eq} & m_b l \\ m_b l & I_{eq} \end{bmatrix} \quad \mathbb{F} = \begin{bmatrix} \frac{2b_w}{r_w^2} & 0 \\ 0 & 0 \end{bmatrix} \quad \mathbb{G} = \begin{bmatrix} 0 & 0 \\ 0 & -m_b g l \end{bmatrix} \tag{25}$$

$\mathbb{H}_T$ and $\overline{u}$ are defined in the equation 18.

The equation 24 can be rewritten in the form:

$$\ddot{\underline{q}} = -\mathbb{E}^{-1}\mathbb{G}\cdot\underline{q} - \mathbb{E}^{-1}\mathbb{F}\cdot\dot{\underline{q}} + \mathbb{E}^{-1}\mathbb{H}_T\cdot\overline{u} \tag{26}$$

Then, with the same state vector defined in the equation 19, one can obtain a state-space representation of the LTI model of the form:

$$\dot{\underline{x}} = \mathbb{A}\cdot\underline{x} + \mathbb{B}\cdot\overline{u} \tag{27}$$

Where,

$$\mathbb{A} = \begin{bmatrix} \mathbb{O}_{2\times2} & \mathbb{I}_{2\times2} \\ -\mathbb{E}^{-1}\mathbb{G} & -\mathbb{E}^{-1}\mathbb{F} \end{bmatrix} \qquad \mathbb{B} = \begin{bmatrix} \mathbb{O}_{2\times2} \\ \mathbb{E}^{-1}\mathbb{H}_T \end{bmatrix} \tag{28}$$

Where $\mathbb{O}_{2\times2}$ is a 2×2 matrix of zeros and $\mathbb{I}_{2\times2}$ is an identity matrix of 2×2.

E. Open-loop stability analysis of LTI model and non-minimum phase system

The poles of the LTI model can be obtained by calculating the eigenvalues of the $\mathbb{A}$ matrix of the equation 27. The system has 4 poles, one at the origin, two negative real ones at -40.3815 and -7.5366, and one positive real one at 8.1626. Having a positive real pole makes the open-loop system an unstable system[10][8], which is correct for having performed the linearization of the model at an operating point corresponding to an unstable equilibrium configuration.

The transfer function obtained for the LTI system from the input T_w to the output x_t is as follows:

$$H(s) = \frac{76.58\cdot s^2 - 3975}{s\cdot(s^3 + 39.76\cdot s^2 - 86.8\cdot s - 2484)} \tag{29}$$

The figure 3 shows the map of poles and zeros for the transfer function $H(s)$.

It should be noted that, in addition to the positive real pole that provides information about the instability of the system, there is a positive real zero that indicates that the system is not of minimum phase (or *non-minimum phase*). This type of systems have different characteristics, among them is that the response to a step presents an initial direction opposite to the one intended by the input[**nonminimumphase**]. In this case, since the closed-loop system still has a positive real-part zero, given a positive x_t^* position setpoint step, the vehicle will initially tend to move in the negative direction of x_t (figure 4).

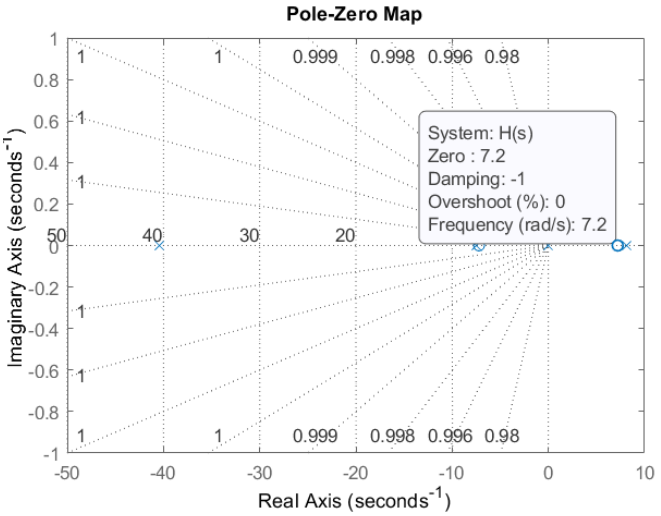

Fig. 3. Map of poles and zeros of the transfer function from T_w to x_t

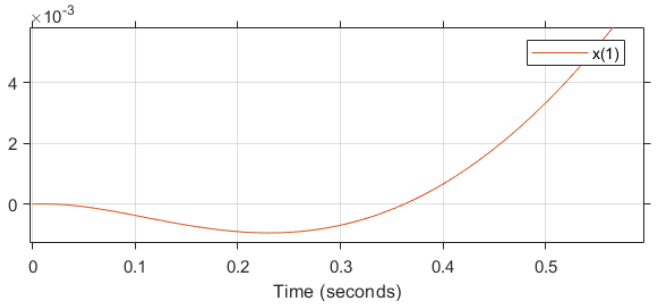

Fig. 4. Initial second enlargement of nonlinear model response with LQG controller

One of the conclusions drawn from this type of behavior is that the response is not instantaneous and makes control more difficult because it is more susceptible to an increase in controller gain.

IV. Sensor and Actuator Modeling

A. Incremental encoder model

The vehicle has an incremental encoder in each of the actuators that allows the angular position of the motor shaft to be known. The encoder generates two square waves 90° out of phase that send 12 pulses for each motor revolution. As shown in the figure 5, different accuracies can be obtained according to how the pulses of these waves are counted: 12 pulses per revolution if only the rising edge of wave A is considered, 12×2 if the rising edge of both waves is considered and 12×4 if in addition to the rising edge the falling edge is considered.

The encoder action is modeled as a quantization of the signal ϕ_m, which if measured in radians will be given by a Δ equal to:

$$\Delta = \frac{2\pi}{12\times4} \tag{30}$$

The difference with a conventional quantization that must be bridged for encoder modeling is that it is not a rounding

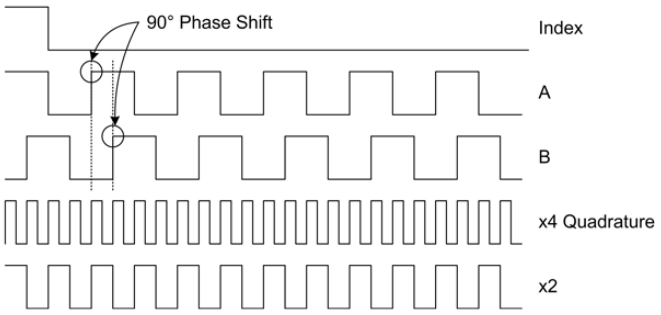

Fig. 5. Quadrature encoder-generated square waves in quadrature

operation, but a ceiling or floor function depending on the direction of rotation of the axis. With $\lceil\rceil$ being the notation for the ceiling function and $\lfloor\rfloor$ being the notation for the floor function, the following quantization function Q is proposed:

$$Q(\phi_m) = \begin{cases} \Delta \cdot \lceil \frac{\phi_m}{\Delta} \rceil & \text{if } \dot{\phi}_m < 0 \\ \phi_m & \text{if } \dot{\phi}_m = 0 \\ \Delta \cdot \lfloor \frac{\phi_m}{\Delta} \rfloor & \text{if } \dot{\phi}_m > 0 \end{cases} \tag{31}$$

The model in MATLAB Simulink is implemented with a function that executes the equation 31. In the figure 6 is the proposed model and in the figure 7 an example of the behavior that presents the proposed quantization for an encoder reading of 12 pulses per revolution in order to have a higher Δ that is easy to observe.

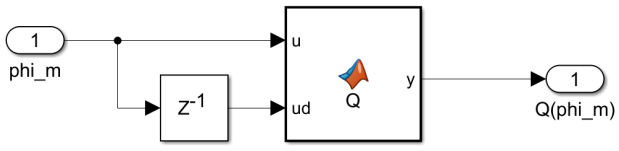

Fig. 6. MATLAB Simulink model of signal quantization ϕ_m

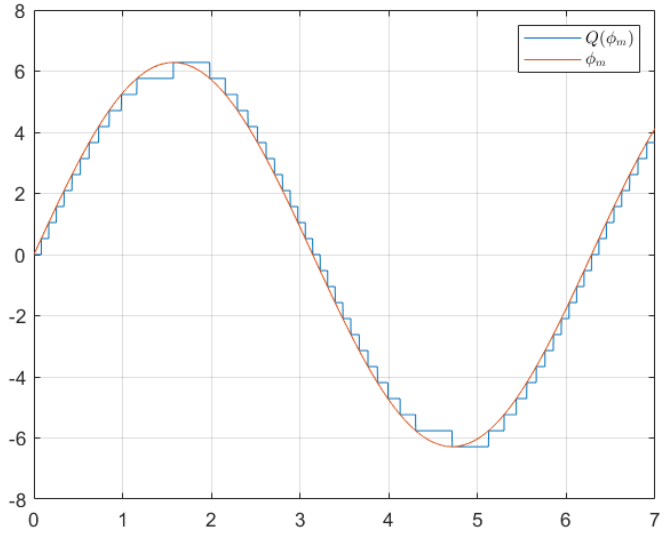

Fig. 7. Example of proposed quantization to emulate quadrature encoder behavior

The advantage of modeling the encoder as a quantization process is that it gives the possibility to apply the theory about the error that the process adds to the signal. Assuming that the probability of the quantization error has uniform distribution[12][17], it can be obtained that the variance of the error is:

$$\sigma_Q^2 = \frac{\Delta^2}{12} \tag{32}$$

It should be noted that, since to emulate the behavior of the encoder the value is not rounded but a ceiling or floor function is applied depending on the direction of rotation of the axis, the average of this probability is not at 0 as in a conventional quantification, but at:

$$\mu_Q = \begin{cases} +\frac{\Delta}{2} & \text{if } \dot{\phi}_m < 0 \\ -\frac{\Delta}{2} & \text{if } \dot{\phi}_m > 0 \end{cases} \tag{33}$$

B. MEMS gyroscope model

As previously mentioned, the inertial measurement unit available in the vehicle contains a gyroscope that allows the measurement of the tilt angular velocity $\dot{\theta}(t)$. Based on the data from the MPU6050 IMU, the model was obtained in MATLAB Simulink Simulink in Figure 22.

It can be seen that the input to the model is the actual sensed angular velocity of the system at the position where the gyro is located. In the mechanical design it was placed such that the y axis of the IMU is parallel to the axis of the wheels, and is in the same vertical plane from which θ is measured, so the measurement of θ is direct. The output of the model is a 16-bit signed integer. The x and z axes of the gyro are not used in this work.

The conversion ratio between the physical measurement in $sfrac°s$ to its representation in a 16-bit signed integer is called the sensitivity factor. For the unit under analysis the full scale range of measurement, which determines the sensitivity, can be set to 4 values: ± 250, ± 500, ± 1000 or $\pm 2000 ^{\circ}/_{s}$. The highest possible sensitivity is desired without saturating the measurement, so the angular velocity of the system is simulated and studied with the full state feedback controller obtained in section V-B under the same perturbation with which the controller was analyzed.

In figure 8 it can be observed that the maximum angular velocity acquired by the vehicle is close to $200 ^{\circ}/_{s}$, so it is considered that by configuring the gyroscope in a range of $\pm 250 ^{\circ}/_{s}$ the measurement will not be saturated. For such a range the sensitivity factor is $131 ^{LSB}/_{(^{\circ}/_{s})}$ (LSB per least significant bit). The nonlinearity of the gyro according to the specifications is 0.2% of full scale, in this case that error will only be $0.5 ^{\circ}/_{s}$.

The device is a MEMS (micro-electromechanical system) gyroscope, whose operating principle is that of an oscillating mass reacting by corioliscite[18] effect and therefore its dynamics can be modeled as a mass-spring system. The manufacturer provides the mechanical frequency of such a system, for the y-axis equal to $\omega_N = 27kHz$ (at least which is the worst case). No damping information is available, so the system is modeled

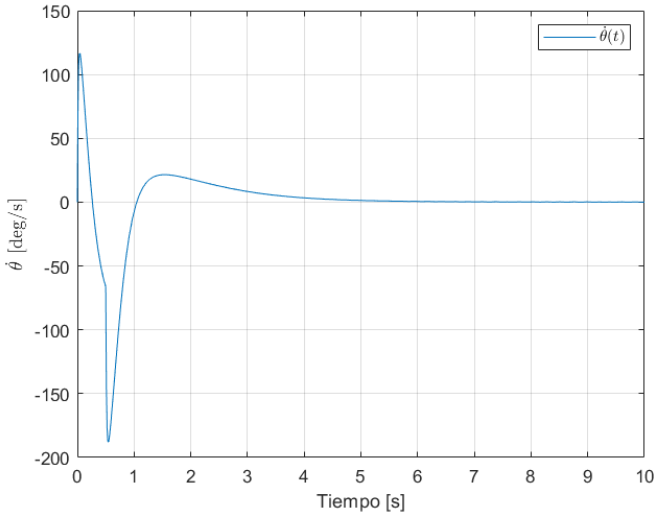

Fig. 8. Response $\dot{\theta}(t)$ of nonlinear system with LQR controller to $10N$ thrust at center of mass for $0.5s$

as a second-order Butterworth filter, where the damping is $\zeta = \sqrt{2}/2$ and the transfer function is of the form,

$$H(s) = \frac{\omega_N^2}{s^2 + 2\zeta\omega_N s + \omega_N^2} \tag{34}$$

The dynamics of the sensor has a much higher frequency than that of the vehicle, therefore it does not affect the measurement and could be neglected.

The device is also subject to a static bias or offset, which can be generated for example by residual voltages on the printed circuit board assembly. This offset can be corrected when starting the vehicle software in the calibration process, it is placed in the model but for simplicity it is given a value of 0.

Like any sensor, the gyro adds noise to the signal. The noise is modeled as white Gaussian noise, i.e., it has mean $\mu_{\text{gyro}} = 0$, same intensity at different frequencies, and therefore constant power spectral density. The sensor specifications provide the information of such noise in amplitude spectral density, equal to $0.005^{\circ}/s/\sqrt{Hz}$ at $10Hz$. It can be obtained in terms of power spectral density by squaring it[15]. Using MATLAB, the signal with noise was simulated and the sensor variance was obtained.

$$\sigma^2_{\text{gyro}} \approx 7.64 \times 10^{-6} \tag{35}$$

Finally, it is important to note that a 16-bit signed integer conversion block was used in the model. In this conversion, a saturation is also performed according to the representation and the chosen scale.

C. Model of accelerometer as a θ sensor

The IMU MPU6050 has a built-in accelerometer in addition to the gyroscope. This allows measuring linear accelerations in its three axes considering the acceleration of gravity. Since gravity is an acceleration that always acts perpendicular to the ground, it can be decomposed in the three axes of the accelerometer and thus, by means of trigonometric identities, the orientation of the sensor can be known. If used in this way, it should be noted that any acceleration caused in the sensor that is not due to gravity will be considered noise as it will skew the measurement.

To estimate the tilt angle θ of the vehicle only two axes of the sensor are used, z aligned with the inverted pendulum and x perpendicular to it and the axis of the wheels, these axes form the plane of the schematic 1. The model obtained for the accelerometer is equivalent to the gyroscope model without the dynamics of the mass-spring system, and can be seen in figure 23.

The input to the model is the actual acceleration measurement on the corresponding axis, and the output in its 16-bit signed integer representation.

The scale range of the accelerometer can be set to ± 2, ± 4, ± 8 or $\pm 16g$. Since it is only desired to read the acceleration of gravity, it is set to $\pm 2g$ even though experiencing other accelerations may cause the measurement to saturate. For the chosen range the sensitivity factor is $16.384^{LSB}/_{g}$.

There is a static offset, but as for the gyroscope in the model it is considered null. The noise incorporated to the reading by the accelerometer has an amplitude spectral density of $400^{\mu g}/\sqrt{Hz}$ and its sampling frequency is $1kHz$ with the possibility of configuring it to obtain readings at a lower frequency.

Using MATLAB, the signal was simulated with noise and the variance of the sensor was obtained.

$$\sigma^2_{\text{accel}} \approx 1.6 \times 10^{-4} \tag{36}$$

$$\sigma^2_{accel} = \left(400\frac{\mu g}{\sqrt{\text{Hz}}}\right)^2 \cdot 10\text{Hz} = 1.6 \times 10^{-6} g^2 \tag{37}$$

However, it is desired to obtain the variance of the θ signal which is the variable to be measured. Therefore, a simulation was implemented where the composition of θ with both accelerations is performed through the function *atan2* and the following variance was obtained:

$$\sigma^2_{\theta} \approx 0.065 \tag{38}$$

D. Direct current motors with gearbox

In the present work we seek to obtain a controller with an independent analysis of the electric motors that will drive the vehicle. However, in order to have a reference and that the control actions are not excessive, the torque modulator is modeled as a first order system with transfer function:

$$H_T(s) = \frac{T_m}{T_m^*} = \frac{1}{\tau s + 1} \tag{39}$$

Where τ is the time constant of the modulator and is taken to be $5ms$.

The motors are considered to have a gearbox with a gear ratio of $1 : 34$. To limit the torque, a saturation block is placed in the model that allows the drives a maximum torque of $8.5 \times 10^{-3}\text{Kg}m$. In addition, it is permanently controlled in the obtained responses that the angular velocity at the output of the gearbox does not exceed 110rpm.

V. Complete state feedback controller design

A. System controllability analysis

The controllability study of the system allows to establish the possibility of locating the eigenvalues or poles of the feedback LTI model[10][2] using a control law such as the one in the equation 40.

$$u = -\mathbb{K} \cdot \underline{x} \tag{40}$$

That the system is controllable also implies that by manipulating the input appropriately, the system can be driven to a desired state (reachability [3]).

Constructing the controllability matrix $\mathscr{C}$ for the system under study with $n = 4$ as:

$$\mathscr{C} = \begin{bmatrix} \mathbb{B}_1 & \mathbb{A}\mathbb{B}_1 & \mathbb{A}^2\mathbb{B}_1 & \mathbb{A}^3\mathbb{B}_1 \end{bmatrix} \tag{41}$$

Where $\mathbb{B}_1$ is the input matrix of the system for the manipulated variable $u = T_w$, its rank can be analyzed, and being equal to 4 it can be confirmed that the system is controllable.

If the system is controllable, as a consequence of everything previously mentioned, the system is also stabilizable, i.e., the eigenvector associated to the positive real pole calculated in section III-E lies within the vector subspace of the controllability matrix.

By establishing the controllability of the system we also verify that the conceptual mechanical design of the robot, more specifically the $\mathbb{B}_1$ matrix of the model, is adequate.

B. LQR linear quadratic controller design

The closed-loop system expression is obtained by replacing the control law of equation 40 in the LTI model of equation 27:

$$\dot{\underline{x}} = \mathbb{A} \cdot \underline{x} + \mathbb{B}_1 \cdot (-\mathbb{K} \cdot \underline{x}) \quad \Rightarrow \quad \dot{\underline{x}} = (\mathbb{A} - \mathbb{B}_1\mathbb{K}) \cdot \underline{x} \tag{42}$$

Where $\mathbb{K}$ is a matrix with as many columns as n order of the model and contains the constants of the controller. These constants are selected such that the eigenvalues of the closed-loop dynamics matrix $(\mathbb{A} - \mathbb{B}_1 mathbbK)$ are in the desired location. Figure 9 shows the full state feedback controller model interacting with the LTI model of the system.

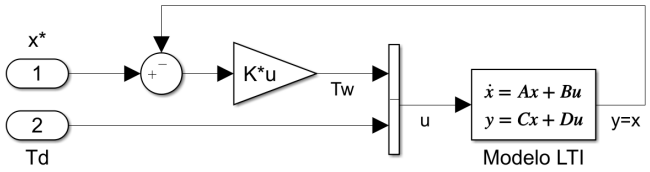

Fig. 9. Complete state feedback controller model in MATLAB Simulink

At a minimum you want the poles to be negative real to have a controller that stabilizes the system. For example, by assigning the poles of the system such that the positive real pole calculated in section III-E is now at -80 and the rest at their original location, the following controller $\mathbb{K}$ is obtained:

$$\mathbb{K} = \begin{bmatrix} 0 & -2.4352 & -1.5771 & -0.2983 \end{bmatrix} \tag{43}$$

And simulating the controller in conjunction with the LTI model of the system, as shown in figure 9, with a perturbation corresponding to $10N$ at the center of mass of the vehicle, so as to push it for half a second, and state setpoint at 0, the response of the figure 10a is obtained. It can be seen that by assigning the poles manually the setpoint is achieved, except for $x_t(t)$ since the system does not return to the initial position.

It is desired that this location of the eigenvalues is performed following an optimal criterion for the model. One of the main reasons is that an excessively fast response leads to excessive stress on the vehicle's actuators.

To find the optimal location of the eigenvalues of the feedback system, a linear quadratic regulator (LQR) is used. The LQR controller is based on minimizing a cost function J that penalizes to a greater or lesser extent the deviation of the system state from the target and the effort admitted in the control input or action[11][6].

$$J = \int_0^\infty \left(\underline{x}^T \mathbb{Q}_x \underline{x} + \underline{u}^T \mathbb{Q}_u \underline{u} \right) dt \tag{44}$$

In the equation 44 we can observe the cost function to be optimized in the LQR control, where $\mathbb{Q}_x$ is the state cost matrix, positive definite matrix, and $\mathbb{Q}_u$ is the control action cost matrix, positive semi-definite matrix. The solution of the LQR problem is given by:

$$\mathbb{K} = \mathbb{Q}_u^{-1} \mathbb{B}_1^T \mathbb{S} \tag{45}$$

Where $\mathbb{S}$ is a positive definite symmetric matrix obtained by solving the algebraic Riccati[11] equation:

$$\mathbb{A}^T\mathbb{S} + \mathbb{S}\mathbb{A} - \mathbb{S}\mathbb{B}_1\mathbb{Q}_u^{-1}\mathbb{B}_1^T\mathbb{S} + \mathbb{Q}_x = 0 \tag{46}$$

The equation 46 is solved by means of software tools, in this case MATLAB.

Then, the LQR controller tuning is done by choosing the weights of the cost matrices $\mathbb{Q}_x$ and $\mathbb{Q}_u$. It is usually by trial and error, however there are different methods to obtain initial values to iterate with. In this work we used a diagonal weighting following Bryson's rule. Diagonal weighting consists of posing diagonal cost matrices, and choosing the elements of the diagonal based on how much each state variable and each corresponding input contributes to the total cost. Being a system of 4 state variables ($n = 4$) and a single manipulated input ($p = 1$), such matrices will be of the form of the equation 47.

$$\mathbb{Q}_x = \begin{bmatrix} q_1 & 0 & 0 & 0 \\ 0 & q_2 & 0 & 0 \\ 0 & 0 & q_3 & 0 \\ 0 & 0 & 0 & q_4 \end{bmatrix} \qquad \mathbb{Q}_u = \begin{bmatrix} \rho_1 \end{bmatrix} \tag{47}$$

Bryson's rule allows setting maximum values for the error of the state variables and maximum values for the stress of the inputs. The weighting is chosen such that $q_i = \alpha_i^2 / x_{i,max}^2$ and $\rho_i = \beta_i^2 / u_{i,max}^2$, where $x_{i,max}$ represents the maximum error allowed for state variable i and $u_{i,max}$ the maximum effort for input i. α_i and β_i are selected such that:

$$\sum_{i=1}^{n} \alpha_i^2 = 1 \qquad \sum_{i=1}^{p} \beta_i^2 = 1 \tag{48}$$

The α_i are assigned a value such that they are all equal, that is $\alpha_i = \sqrt{0.25}$ such that when added to the square they result in 1. For the translation variable x_t a maximum error of

$0.01m$ and the maximum translation speed error of $0.0151m/s$ was assigned. The maximum allowable tilt angle posed was $20°$ and the maximum tilt angular velocity error of $1rpm$, both relatively large to allow for a translation variable correction. If such constraints are too aggressive the tilt angle will always be very close to 0 and vehicle motion is prevented.

For the control action cost matrix $\mathbb{Q}_u$ the parameter β_1 is equal to 1. With u being the sum of the torque of the two actuators, $u_{1,max}$ is chosen as 2 times 90% of the maximum load torque of the motors which is $8.5 \times 10^{-3} Kg \cdot m$ according to the technical specifications. Therefore, $u_{1,max} = 0.0153$ and $\rho_1 = 4.2719 \times 10^3$. The resulting cost matrices are as follows:

$$\begin{aligned} \mathbb{Q}_x &= \begin{bmatrix} 2.5 & 0 & 0 & 0 \\ 0 & 0.0021 & 0 & 0 \\ 0 & 0 & 1.0994 & 0 \\ 0 & 0 & 0 & 0.0228 \end{bmatrix} \\ \mathbb{Q}_u &= \begin{bmatrix} 4.2719 \times 10^3 \end{bmatrix} \end{aligned}$$

It is important to note that these cost matrices were obtained by regulating the maximum error value of the admitted state variables and the maximum stress value of the input, which is much more intuitive as a designer than locating the poles in the complex plane.

The resulting controller constant matrix is as follows:

$$\mathbb{K} = \begin{bmatrix} -0.7650 & -0.6428 & -0.3304 & -0.1098 \end{bmatrix} \quad (49)$$

The poles with the new constants are located at -75.8387, -0.9645, -3.9077 and -10.6379. Figure 10b shows the response of the LTI model of the vehicle with the LQR controller to a null state setpoint and a perturbation corresponding to a thrust force of $10N$ on the center of mass of the vehicle per half second. It can be seen that compared to figure 10a, a response a few seconds slower but compliant with the return of the vehicle to the origin is obtained.

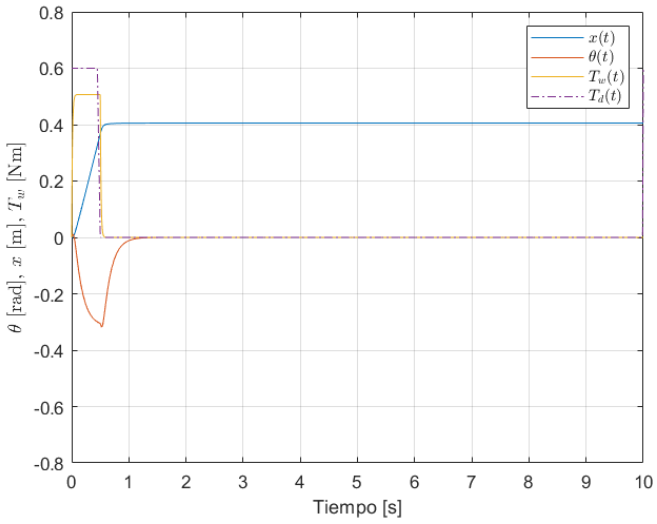

(a) Response with controller with pole mapping

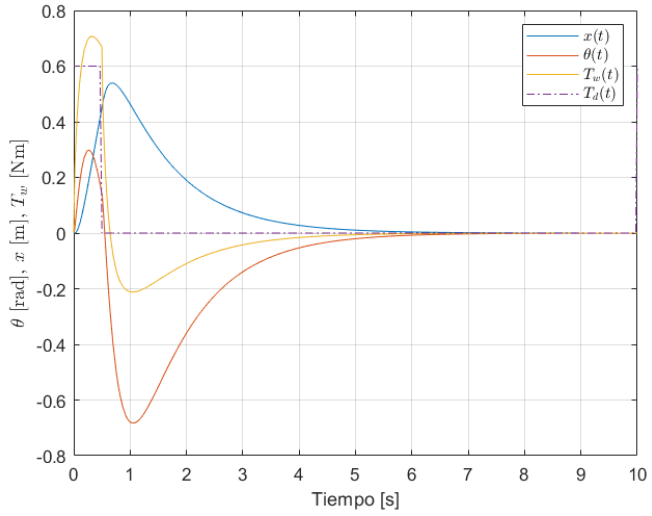

(b) Response with LQR driver

Fig. 10. Response of LTI model with full state feedback controller to $10N$ thrust on vehicle center of mass

C. LQR controller performance evaluation

Once the desired controller is obtained, it is evaluated under the requirements stated in section II. If the requirements are not met, the controller tuning process is iterated again.

With the LQR controller of equation 49 the LTI model meets the setpoint within the imposed tolerances, as does the mechanical model as can be seen in figure 11, where x_t^* is the setpoint to follow and *Vehicle:1(1)* is the translation variable x_t of the mechanical model in Simscape Multibody.

VI. Optimal observer design

A. System observability analysis

In section V-B it was assumed that all system state variables are accessible (see figure 9) which is incorrect since in the actual implementation only a limited amount of such variables are measured with the sensors available in the vehicle. However, the design of the optimal controller by full LQR state feedback is valid, because an estimation of the inaccessible state variables can be made from the measured variables and the control action[13] by means of a so-called closed-loop estimator or observer. The measured variables are represented by the following equation:

$$\underline{y} = \mathbb{C} \cdot \underline{x} \quad (50)$$

Where $\underline{y}$ is a vector of q components (less than n) and $\mathbb{C}$ is the matrix of measured variables.

Similar to the study of controllability in section V-A, the observability of the system is studied. The observability allows to establish the possibility of making a complete estimation of the $\underline{x}$ state of the system from the measurement of the $\underline{y}$ variables.

Constructing the observability matrix $\mathscr{O}$ for the system under study with $n = 4$:

$$\mathscr{O} = \begin{bmatrix} \mathbb{C} \\ \mathbb{C}\mathbb{A} \\ \mathbb{C}\mathbb{A}^2 \\ \mathbb{C}\mathbb{A}^3 \end{bmatrix} \quad (51)$$

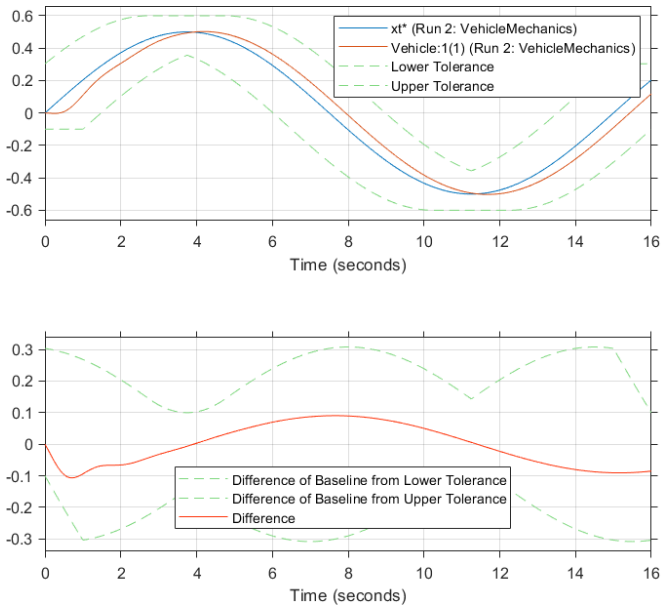

Fig. 11. Setpoint tracking check of mechanical model with LQR controller

Its rank can be analyzed, and being equal to the order of the model, it can be confirmed that the system is observable for the $\mathbb{C}$ matrix considered.

For the system under study, the observability matrix $\mathcal{O}$ has rank equal to 4 if and only if the state variable x_t, i.e., the translation of the vehicle, is measured. Of course, the system is still observable if to this measurement is added the measurement of the tilt angle or the corresponding velocities.

As described in section IV, in the vehicle x_t is indirectly measured through the incremental encoders in the motors measuring ϕ_m, the tilt angular velocity $\dot{\theta}$ is measured with a gyroscope and also the tilt angle θ with an accelerometer by calculating the corresponding trigonometric ratios. So the matrix $\mathbb{C}$ is of the form:

$$\mathbb{C} = \begin{bmatrix} \frac{12\times4\times34}{r_w} & 0 & 0 & 0 \\ 0 & 1 & 0 & 0 \\ 0 & 0 & 0 & 1 \end{bmatrix} \tag{52}$$

That the system is observable not only ensures the ability to "reconstruct" the state of the system from the measured state variables, but also assures us the possibility of assigning the observer's eigenvalues so that such estimation is fast to a greater or lesser extent[7], analogous to the assignment of poles of the closed-loop system with the concept of controllability.

B. Kalman filter design

The observer itself is a linear dynamic system whose inputs are the measured state variables $\underline{y}$ of the system to be observed, and the control action $\underline{u}$ with which that system is manipulated[13][4]. The equation describing the observer's behavior is as follows:

$$\dot{\underline{\hat{x}}} = \mathbb{A} \cdot \underline{\hat{x}} + \mathbb{B}_1 \cdot \underline{u} + \mathbb{L} \cdot (\underline{y} - \underline{\hat{y}}) \tag{53}$$

Where $\underline{\hat{x}}$ is the state estimate, $\underline{\hat{y}}$ is the estimate of measured variables according to the equation $\underline{\hat{y}} = \mathbb{C} \cdot \underline{\hat{x}}$, and where $\mathbb{L}$ is the matrix of constants that allows the observer's eigenvalues to be located such that the estimation error converges to zero in the required time and manner (equivalent to the $\mathbb{K}$ matrix of constants of state feedback control). Working algebraically with the equation 53, one can obtain an equation of the form:

$$\dot{\underline{\hat{x}}} = (\mathbb{A} - \mathbb{L}\mathbb{C}) \cdot \underline{\hat{x}} + \begin{bmatrix} \mathbb{B}_1 & \mathbb{L} \end{bmatrix} \cdot \begin{bmatrix} \underline{u} \\ \underline{y} \end{bmatrix} \tag{54}$$

It can be shown that if the system is observable, making the observer's dynamics stable, or what is the same, choosing the constants of the matrix $\mathbb{L}$ such that the eigenvalues of $(\mathbb{A} - \mathbb{L}\mathbb{C})$ are negative real, then the estimate $\underline{\hat{x}}$ tends to be equal to $\underline{x}$ and, hence, the error tends to zero[4].

The observer implementation in MATLAB Simulink is found in Figure 12. The inputs $\underline{u}$ and $\underline{y}$ are concatenated into an input vector to a state-space model with the dynamics of the observer. In such a model $A = \mathbb{A} - \mathbb{L}\mathbb{C}$, $B = \begin{bmatrix} \mathbb{B}_1 & \mathbb{L} \end{bmatrix}$, C is an identity matrix of 4×4 since the full state estimate is desired as output, and D is a null matrix with number of columns equal to B and number of rows equal to C. The output of the state-space model corresponds to the full state estimate $\underline{x}$.

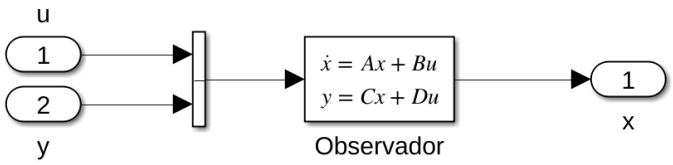

Fig. 12. Observer implementation in MATLAB Simulink

A first observer was implemented by manually assigning the eigenvalues, placing them at -1, -2, -4 and -8. The resulting observer constant matrix $\mathbb{L}$ is as follows:

$$\mathbb{L} = \begin{bmatrix} 0 & 0 & -0.1446 \\ 0 & 8 & 1 \\ 0 & -3.8157 & 5.4771 \\ 0.0003 & 86.8005 & -34.8025 \end{bmatrix} \tag{55}$$

Then the observer with measured outputs was connected with the corresponding noise to the LQR controller obtained in section V-B as seen in figure 25. In this way, the tracking of the state variables against a sinusoidal setpoint of $1m$ amplitude and $15s$ period can be analyzed.

In figure 13 it can be seen that the estimation of $\dot{\theta}$ is not correct, and therefore the system could not be controlled with the $\mathbb{L}$ matrix obtained.

It is desired that, as in pole placement with the LQR controller, the observer poles be optimally assigned. Placing the eigenvalues so that the observer is arbitrarily fast may accentuate the noise and/or disturbances present in the system[9]. The Kalman filter is a complete optimal state observer given some information about the perturbations present in the system and the noise present in the measurements[9].

Defining system disturbances as v, also called process noise, and measurement noise as w, noises with Gaussian distribution and zero mean[14], the new LTI model equations this time instead of stochastic algebraic, are of the form:

$$\begin{cases} \dot{\underline{x}} = \mathbb{A} \cdot \underline{x} + \mathbb{B} \cdot \underline{u} + v \\ \underline{y} = \mathbb{C} \cdot \underline{x} + w \end{cases} \tag{56}$$

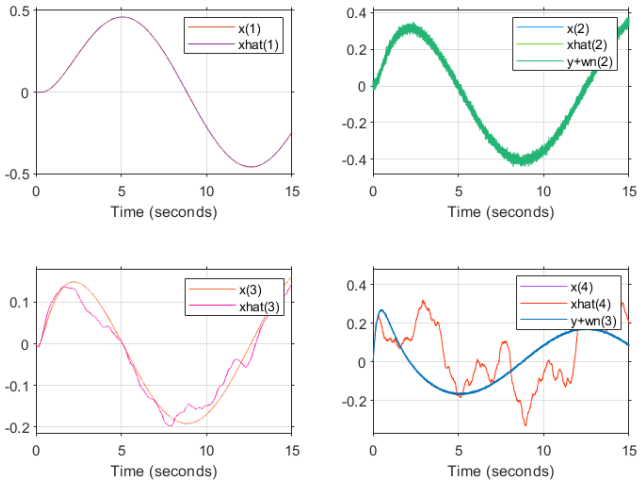

Fig. 13. State estimator connected to controller with full LQR state feedback with sinusoidal position setpoint

Since the estimation error $\underline{\tilde{x}} = \underline{x} - \underline{\hat{x}}$, the dynamic error equation for the Kalman filter will be:

$$\dot{\underline{\tilde{x}}} = (\mathbb{A} - \mathbb{LC}) \cdot \underline{x} + v - \mathbb{L} \cdot w \tag{57}$$

In this case, being a stochastic system we add that if $(\mathbb{A}-\mathbb{LC})$ is stable the estimation error is a stationary stochastic process and the error will have a Gaussian distribution that does not vary in time[14]. The Kalman filter is an optimal estimator by minimizing the variance of the estimation error given by:

$$P_{\tilde{x}} = \mathbb{E}(\underline{\tilde{x}}(t)^T \underline{\tilde{x}}(t)) \tag{58}$$

Where $P_{\tilde{x}}$ is a positive definite symmetric $n \times n$ covariance matrix obtained by solving the following equation:

$$P_{\tilde{x}}(\mathbb{A} - \mathbb{LC})^T + (\mathbb{A} - \mathbb{LC})P_{\tilde{x}} - \mathbb{L}R_w\mathbb{L}^T + R_v = 0 \tag{59}$$

The equation 59 is equivalent to the Riccati equation of the V-B section, so the problem is solved in much the same way as the LQR problem.

By introducing disturbances and noise to the system, the observer design enters into a trade-off relationship where the greater the noise of the measurements made the greater the confidence in the model should be and, vice versa, the greater the process noise the greater the confidence needed in the measurements[9]. This will be adjusted by using the R_v and R_w parameters[14] present in the equation 59 which define the process and measurement noise as follows:

$$\begin{aligned} \mathbb{E}(v(s)v^T(t)) &= R_v \cdot \delta(t-s) \\ \mathbb{E}(w(s)w^T(t)) &= R_w \cdot \delta(t-s) \end{aligned} \tag{60}$$

Where δ is the Dirac Delta function or unit impulse.

If the system is observable, the gain matrix $\mathbb{L}$ solution of the optimal observer problem will be given by:

$$\mathbb{L} = P_{\tilde{x}}\mathbb{C}^T R_w^{-1} \tag{61}$$

As for LQR, the calculation of $\mathbb{L}$ is solved using MATLAB.

The R_v and R_w matrices obtained following the results of the analysis of the IV section are as follows:

$$R_v = 0.1 \qquad R_w = \begin{bmatrix} \sigma_Q^2 & 0 & 0 \\ 0 & \sigma_{\text{accel}}^2 & 0 \\ 0 & 0 & \sigma_{gyro}^2 \end{bmatrix} \tag{62}$$

And it results in a Kalman filter with the following $\mathbb{L}$ matrix:

$$\mathbb{L} = \begin{bmatrix} 0 & -0.0001 & -0.0440 \\ -0.0004 & 0.2148 & 1.0004 \\ 0.2649 & 0.1811 & -4.6997 \times 10^4 \end{bmatrix} \tag{63}$$

The poles of the optimal observer are located at -0.0021, -0.2147, -29.0842 and -1.0691×10^6.

Adequate performance is obtained for both the LTI model and the nonlinear model, the estimation for the same case as above can be seen in figure 14.

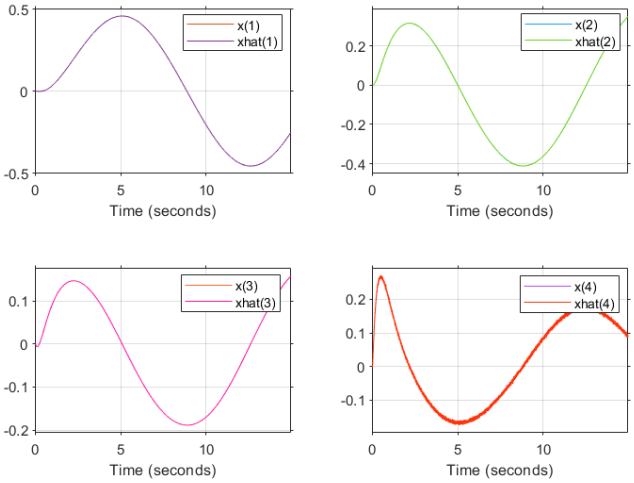

Fig. 14. Controller-connected optimal state estimator with full LQR state feedback with sinusoidal position setpoint

Importantly, not only are the state variables tracked correctly (the curves are overlaid), but the filtering action of the observer can also be observed, removing the high frequency components of the noisy measurement.

C. Performance evaluation of LQR controller with Kalman filter

The fulfillment of the requirements stated in section II of the LQR controller with the full state estimation provided by the obtained Kalman filter is evaluated.

In figure 15 it can be seen that for a sinusoidal position setpoint of $1m$ amplitude and $15s$ period the vehicle respects the imposed tolerances.

VII. LQG CONTROLLER PERFORMANCE ANALYSIS

The results obtained for the LQG controller, i.e., the combination of the linear quadratic regulator LQR and the linear quadratic observer or Kalman filter, on the nonlinear model of the vehicle are shown below.

In figure 16 the response of the controller at different initial angles θ_0 can be observed. The maximum angle at which the controller can stabilize the vehicle is approximately $30°$.

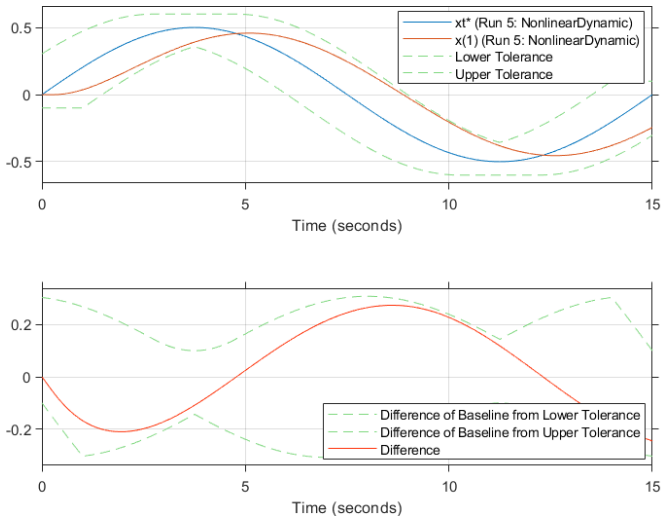

Fig. 15. Setpoint tracking check of nonlinear model with LQR controller and Kalman filter

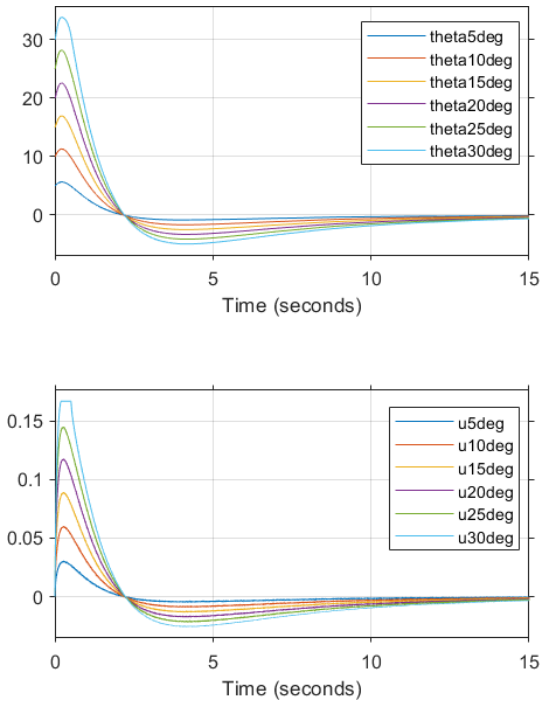

Fig. 16. Maximum stabilizable angle assessment

Figure 17 shows the response of the nonlinear model with the obtained LQG controller to different impulsive thrust forces on the vehicle center of mass. The maximum stabilizable thrust force is about $4N$.

VIII. Simscape Environment for Design Verification

Simscape is a MATLAB Simulink tool where physical systems (whether electrical, mechanical, pneumatic, hydraulic, thermal, etc.) are specifically modeled by interconnecting component blocks without the need to derive mathematical equations from first principles. Simscape Multibody is an extension of the Simscape tool for the analysis, simulation and

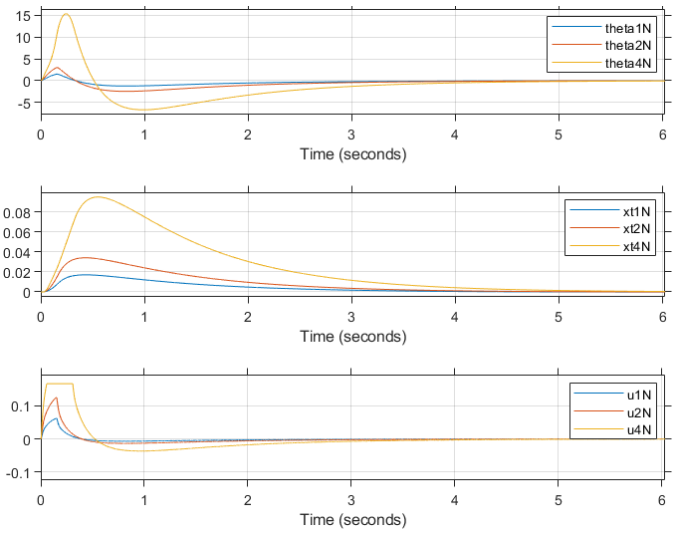

Fig. 17. Stabilizable maximum impulsive thrust force assessment

three-dimensional visualization of mechanical systems, always within the same Simulink development environment.

In this work, Simscape Multibody is used as a validation stage of the design, since the tool will provide a vehicle model that, unlike previous models, is closer to reality by respecting the real mechanical design of the vehicle (importing the corresponding CAD software designs); using a more complex wheel/ground contact model[16] where static and dynamic friction, ground stiffness and damping, friction law, etc. are modeled; and considering aspects that were simplified in the equation-based approach.

The mechanical model of the vehicle, figure 24, was implemented, which has as inputs the torque on the wheels and the perturbation in the form of thrust force on the center of mass of the chassis, and as outputs the actual state of the model ($x_t(t)$, $\dot{x}_t(t)$, $\theta(t)$ and $\dot{theta}(t)$) and the variables needed for the sensor models of the system. The outputs are posed in this way so that the controller can be verified with and without an observer.

For obtaining x_t and $\dot{x}_t$ the following relation is performed:

$$x_t(t) = \frac{q_1 + q_2}{2} \cdot r_w \qquad \dot{x}_t(t) = \frac{\omega_1 + \omega_2}{2} \cdot r_w \tag{64}$$

Where q_1, q_2 are the angular position of wheels 1 and 2, and q_1, q_2 their angular velocity. Position and velocity are averaged since in the paper both wheels were modeled as a single motion but in the simulation environment with Simscape Multibody their motion is independent.

To identify the rest of the necessary variables, a transformation sensor block was implemented, which reads the changes in both rotation and translation of a reference system in the vehicle chassis with respect to the reference system of the environment. Using this transformation allows establishing an equivalence between the reference system in the chassis with the reference system of the inertial measurement unit, so that the angular velocities and linear accelerations measured by the transformation emulate those acquired by the sensor, see figure 18.

For the output read by the gyroscope only a conversion from $^{rad}/_{s}$ to $^{\circ}/_{s}$ is performed. For the accelerometer output

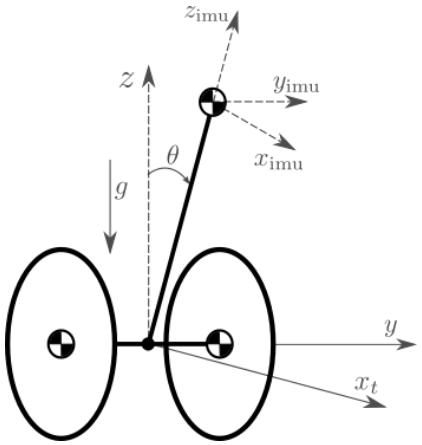

Fig. 18. Physical system scheme with inertial measurement unit reference system

it is necessary to incorporate the decomposition of the vector associated with the acceleration of gravity to the corresponding linear accelerations, and perform the conversion from $^{m}/_{s^2}$ to g. This can be seen in figure 19, where R is the rotation matrix of the vehicle chassis with respect to the surrounding reference frame.

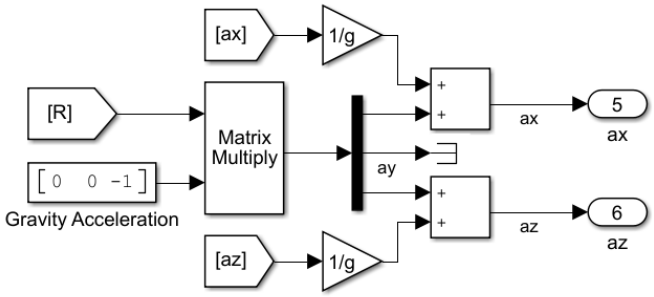

Fig. 19. Interface of the mechanical model of the vehicle to accelerometer reading

IX. Conclusions

One of the great advantages provided by the proposed optimal controller design is that once the linear quadratic regulator LQR and the linear quadratic observer (or Kalman filter) are obtained separately, when combined they are still optimal[5].

A LQG controller was implemented and when interacting with the LTI model of the vehicle it performs adequately meeting the requirements imposed. The same happens when placing the same controller in the non-linear model of the vehicle. In the case of the mechanical model with Simscape Multibody, which is supposed to be closer to reality because of everything described in the section VIII, the response of the linear quadratic controller is more oscillatory than in the linear model, which implies greater instability and large differences with the mathematical model proposed that the controller cannot bridge. Even so, the LQR controller meets the requirements. The difficulty arose when implementing the linear quadratic observer on the mechanical model. In spite of performing successive iterations on the adjustment of the R_v and R_w matrices, the Kalman filter gave good performance in the estimation of x_t or in θ and $\dot{theta}$ but it was not possible to comply with all the state variables. It is necessary to continue the study with a robustness analysis of the controller, making the necessary modifications to be able to bridge the uncertainties of the model. Otherwise, it is necessary to make modifications to the mathematical model to bring it closer to the real behavior of the vehicle.

Another important observation is the delay that the system presents to the setpoint tracking because it is a non-minimum phase system. One of the possible solutions that can be proposed to improve this characteristic is the implementation of a direct control loop or *feedforward*.

Despite not having been able to obtain a controller that performs adequately on the mechanical model of the vehicle, a systematic analysis for the implementation of a LQG controller in this type of vehicle was successfully developed.

References

[1] Brian D. O. Anderson and John B. Moore. *Optimal Control: Linear Quadratic Methods*. Dover Publications, Inc., 2007. ISBN: 9780486457666.

[2] Steven L. Brunton. *Controllability*. URL: https://www.youtube.com/watch?v=1YMTkELi3tE&list=PLMrJAkhIeNNR20Mz-VpzgfQs5zrYi085m&index=5.

[3] Steven L. Brunton. *Controllability, Reachability, and Eigenvalue Placement*. URL: https://www.youtube.com/watch?v=1YMTkELi3tE&list=PLMrJAkhIeNNR20Mz-VpzgfQs5zrYi085m&index=6.

[4] Steven L. Brunton. *Full-State Estimation*. URL: https://www.youtube.com/watch?v=1YMTkELi3tE&list=PLMrJAkhIeNNR20Mz-VpzgfQs5zrYi085m&index=17.

[5] Steven L. Brunton. *Linear Quadratic Gaussian (LQG)*. URL: https://www.youtube.com/watch?v=1YMTkELi3tE&list=PLMrJAkhIeNNR20Mz-VpzgfQs5zrYi085m&index=18.

[6] Steven L. Brunton. *Linear Quadratic Regulator (LQR) Control for the Inverted Pendulum on a Cart*. URL: https://www.youtube.com/watch?v=1YMTkELi3tE&list=PLMrJAkhIeNNR20Mz-VpzgfQs5zrYi085m&index=14.

[7] Steven L. Brunton. *Observability*. URL: https://www.youtube.com/watch?v=1YMTkELi3tE&list=PLMrJAkhIeNNR20Mz-VpzgfQs5zrYi085m&index=16.

[8] Steven L. Brunton. *Stability and Eigenvalues*. URL: https://www.youtube.com/watch?v=h7nJ6ZL4Lf0&list=PLMrJAkhIeNNR20Mz-VpzgfQs5zrYi085m&index=3.

[9] Steven L. Brunton. *The Kalman Filter*. URL: https://www.youtube.com/watch?v=1YMTkELi3tE&list=PLMrJAkhIeNNR20Mz-VpzgfQs5zrYi085m&index=18.

[10] Steven L. Brunton and J. Nathan Kutz. *Data Driven Science and Engineering*. 2017. Chap. Dynamics and Control.

[11] Rodrigo Gonzalez. *Controlador LQR en espacio de estados*. URL: https://www.youtube.com/watch?v=DXZjpnBsvDo&t=1s.

[12] Rodrigo Gonzalez. *Conversión Analógica/Digital*. URL: https://www.youtube.com/watch?v=kAHE7barzCU.

[13] Rodrigo Gonzalez. *Estimación de estados*. URL: https://www.youtube.com/watch?v=49PpBKBdLsg.

[14] Rodrigo Gonzalez. *Filtro de Kalman*. URL: https://www.youtube.com/watch?v=ac4QxCK-XYg.

[15] G. Heinzel, A. Rüdiger, and R. Schiling. "Spectrum and spectral density estimation by the Discrete Fourier-transform (DFT), including a comprehensive list of windowfunctions and some new flat-top windows." In: (Feb. 2002).

[16] Steve Miller. *Simscape Multibody Contact Forces Library*. July 2021. URL: https://github.com/mathworks/Simscape-Multibody-Contact-Forces-Library/releases/tag/21.1.5.0.

[17] Lizhe Tan and Jean Jiang. *Digital Signal Processing*. Third Edition. 2019. Chap. Signal Sampling and Quantization.

[18] Jeff Watson. *MEMS Gyroscope Provides Precision Inertial Sensing in Harsh, High Temperature Environments*. URL: https://www.analog.com/en/technical-articles/mems-gyroscope-provides-precision-inertial-sensing.html.

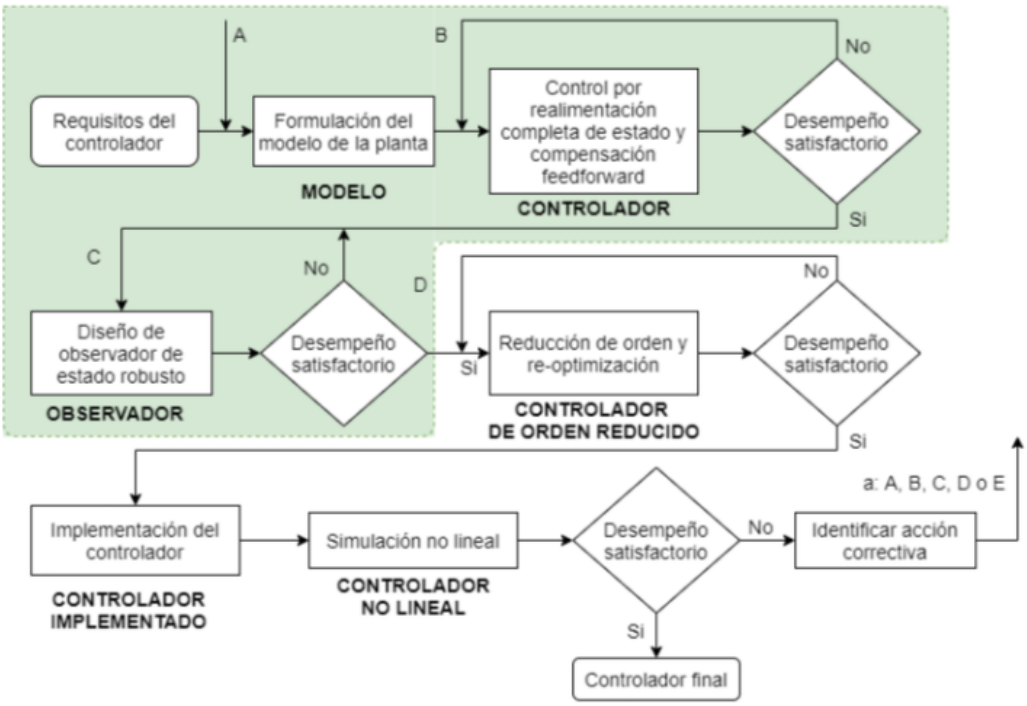

Fig. 20. Controller design process

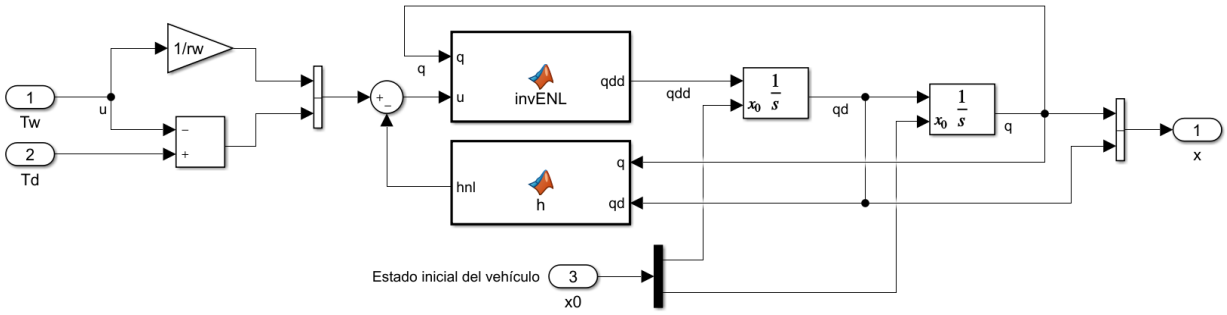

Fig. 21. Nonlinear Model in MATLAB Simulink

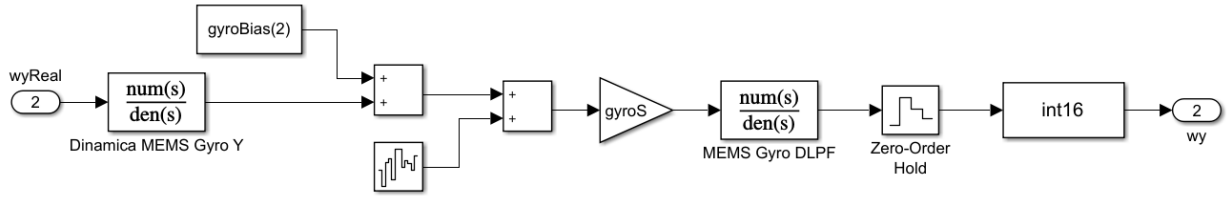

Fig. 22. Model gyroscope for angular rate measurement $\dot{\theta}(t)$

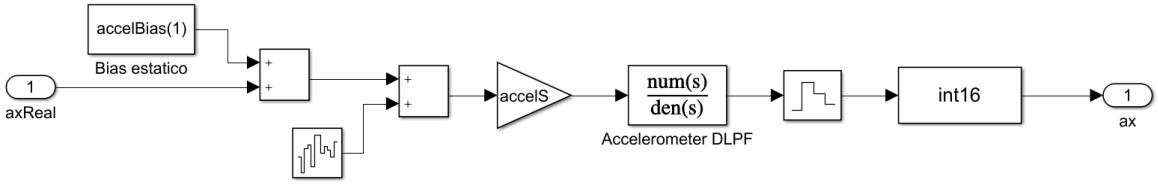

Fig. 23. Accelerometer model for tilt angle measurement $\theta(t)$

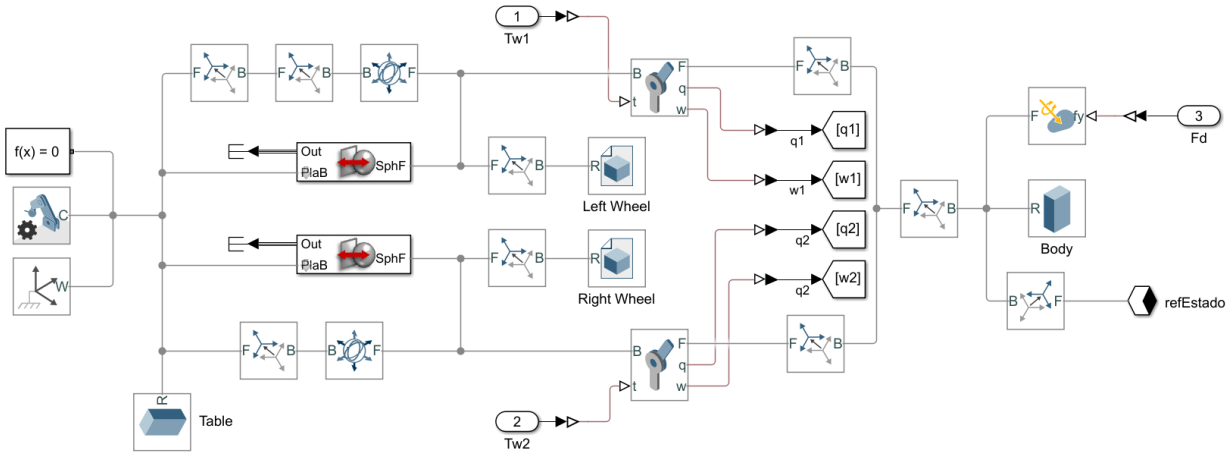

Fig. 24. Mechanical model of the vehicle with Simscape MultibodySimulink

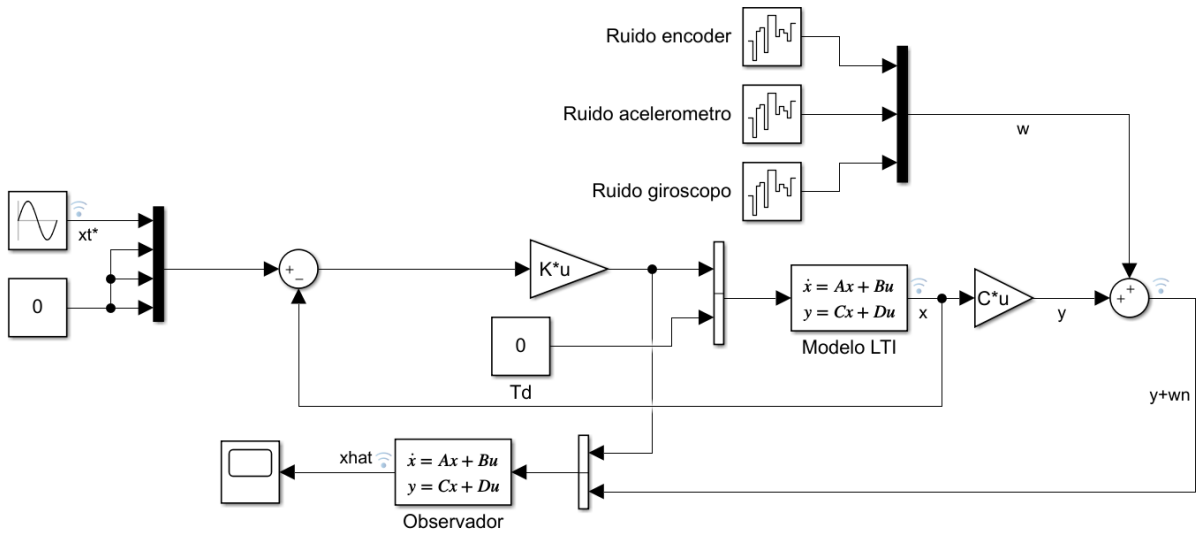

Fig. 25. Observation of LQR controller state variables at sinusoidal position setpoint in LTI model

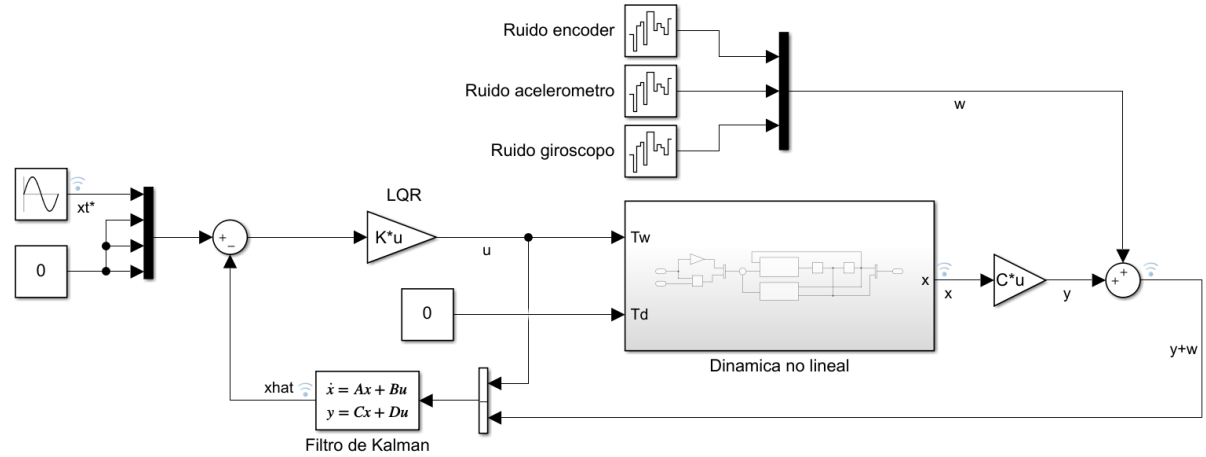

Fig. 26. LQR controller plus Kalman filter on nonlinear system against sinusoidal position setpoint